14

Underground Mining

14.1 Introduction

The mechanical problem in underground mining is that the stope and laneway are always in a state of dynamic evolution, induced by stress adjustment that is caused by excavation and shocks. The dynamic evolution induces a crack field in the wall rock expansion and in the end it caves in. So the mechanics problem in mining is different from other rock engineering problems, such as in powerhouse construction of a hydroelectric power station, traffic tunneling, national defense engineering of rock, etc., which will be firmly supported as soon as they are excavated. However, in mining, the evolution of the crack field and the caving in of the rock are fully used in ore extraction and ground pressure control, such as the mining methods of block caving and long wall mining. In the block caving method, the mining block is undercut near its bottom in order to expose a large free surface near which the ore is in a state of tension, so that cracks in the ore body expand, run through and induce ore caving, as shown in Fig. 14.1 and Fig. 14.2 (Brown, 2003).

In the long wall mining method, see Fig. 14.3 and Fig. 14.4, when the worked-out section is too large, the work face will bear too great a pressure and the sudden rupture of the roof will cause a great shock to the support system. So an ideal mode is that, as the work face advances, the roof caves in bit by bit, which will relief the stress on the work face and avoid the sudden rupture of the roof. It is very necessary in the two mining methods to predict the evolution of the crack field in the wall rock. That is the important mechanical problem in underground mining.

This chapter is contributed by Professors Wang L, Henan Technical University, Jiaozuo, China and Gao Q, Key Laboratory of Ministry of Education for Highly Effective Mining and Safety in Metal Mines; Beijing; China and Beijing Science and Technical University, Beijing, China

M.-H. Yu et al., *Computational Plasticity*

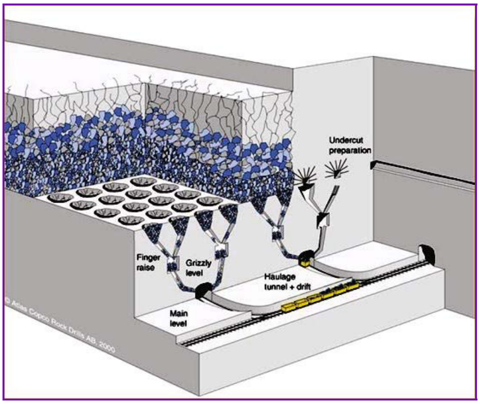

Fig. 14.1 Model of block caving (Brown, 2003)

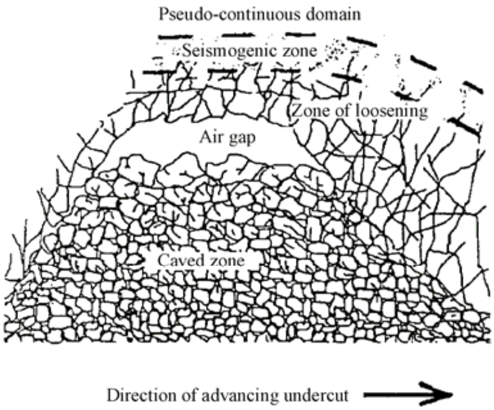

Fig. 14.2 Caving process zone expanding with advancing undercut

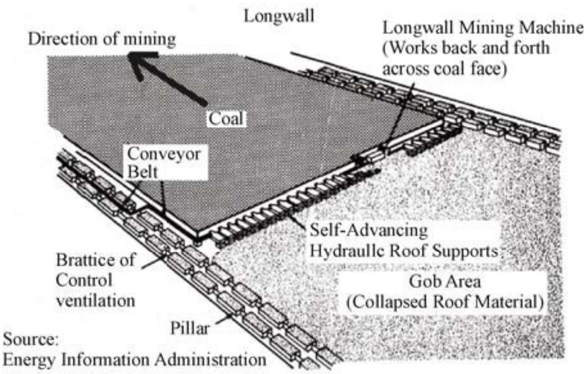

Fig. 14.3 Model of long wall mining

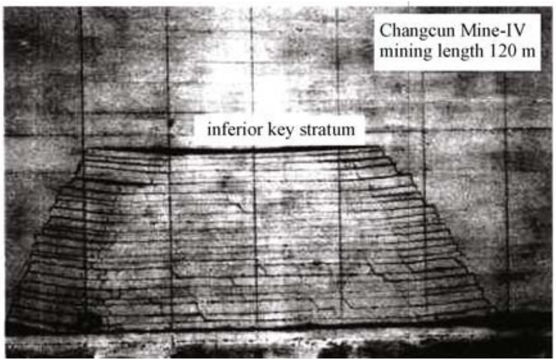

Fig. 14.4 Crack field expanding with extraction advancing

In the calculation of the fracture zone, it is an important problem to select the fracture rule for the rock, which involves choosing a reasonable strength theory. Though strength theory is one of the earliest classic problems in mechanics, it is still progressing. So far, there have been over a hundred mathematics models or criteria proposed. They are divided into single-shear strength theory, twin-shear strength theory and three-shear strength theory under the framework of the unified strength theory. The single strength theory does not consider the effect of intermediate principal stress σ_2, it expresses the stress function of materials with the shear stress and normal stress on the maximum shearing plane, e.g. the Mohr-Columb strength criterion and Tresca strength criterion. Three-shear strength theory is also called octahedral strength theory, e.g. Huber-von Mises criterion and Drucker Prager criterion. Twin-shear theory was proposed by Yu in 1961, 1983 and 1985.

In 1991, Yu presented the unified strength theory in Tokyo and then, in 1992 and in 1994, he gave a further discourse of his theory. The unified strength theory has the advantage that it reflects not only the effects of the intermediate principal stress on material yielding but also the transition from the stress state of generalized tension to that of generalized compression with the intermediate principal stress increasing from $\sigma_2=\sigma_3$ to $\sigma_2=\sigma_1$ in its two expressions (Yu, 1998; 2004).

In this chapter, two examples of the application of the unified strength theory in underground mining are introduced. Block caving and long wall mining are described. In order to reflect the evolution of the crack field in the wall rock, an elastic-brittle damage model has to be established first.

14.2 Elastic-Brittle Damage Model Based on Twin-Shear Theory

14.2.1 Damage Model

The damage variable is defined as

$$D = \left(\varepsilon / \varepsilon_s \right)^n \tag{14.1}$$

where ε_s represents the strain when the material is fully fractured, corresponding to D=1; ε is the elastic strain and n is the brittle exponent. The meaning of the damage parameters is shown in Fig. 14.5. They have different values under uniaxial tension and compression.

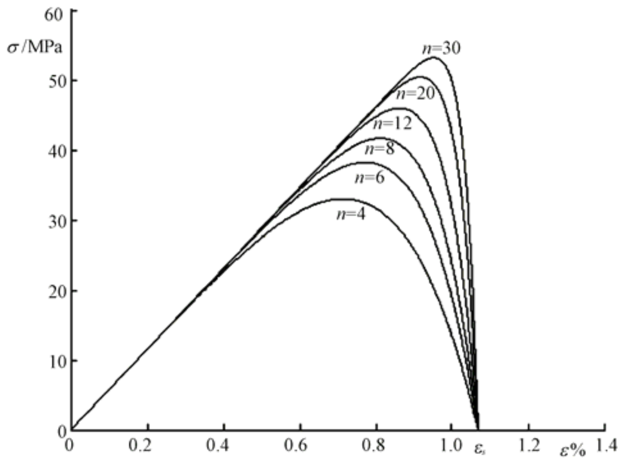

Fig. 14.5 Stress-strain curves of elasto-brittle rock at different n

14.2.2 Three-Dimensional Damage Model

According to twin-shear strength theory (Yu, 1985), the complex stress state can be divided into two kinds of equivalent uniaxial stress states, which are equivalent tension and equivalent compression. The twin-shear strength theory is generalized into a 3D damage model in this research. The twin-shear damage surface equations with principal strains are defined as

$$F' = \left[\varepsilon_1 - \frac{1}{2}(\varepsilon_2 + \varepsilon_3)\right] + \frac{(1-\alpha)(1+\nu)}{(1+\alpha)(1-\nu)}\left[\varepsilon_1 + \frac{1}{2}(\varepsilon_2 + \varepsilon_3)\right] = \frac{2(1+\nu)\varepsilon'_c}{1+\alpha}$$

$$\text{When } \varepsilon_2 \le \frac{\varepsilon_1(1-\alpha\nu) + \varepsilon_3(\alpha-\nu)}{(1-\nu)(1+\alpha)} \text{ (generalized tension)} \tag{14.2a}$$

$$F = \left[\frac{1}{2}(\varepsilon_1 + \varepsilon_2) - \varepsilon_3\right] + \frac{(1-\alpha)(1+\nu)}{(1+\alpha)(1-\nu)}\left[\frac{1}{2}(\varepsilon_1 + \varepsilon_2) + \varepsilon_3\right] = \frac{2(1+\nu)\varepsilon'_c}{1+\alpha}$$

$$\text{when } \varepsilon_2 \ge \frac{\varepsilon_1(1-\alpha\nu) + \varepsilon_3(\alpha-\nu)}{(1-\nu)(1+\alpha)} \text{ (generalized compression)} \tag{14.2b}$$

where $\alpha = \varepsilon_c^t / \varepsilon_c^c$. ε_c^c, ε_c^t represent the critical value of materials yielding under uniaxial compression or uniaxial tension, they are always positive in the expressions.v is the Poisson rate; the expression to the right of Eqs. (14.2a) and (14.2b) can be simplified into a material parameter C. When the strain state is within the damage surface, that is when $|F|<|C|$ or $|F'|<|C|$, there is no damage evolution. If not, damage evolves. With damage evolution, damage surfaces will shrink because of softened material, so the material parameter C will become small. The 3D damage model can be established by F or F' tracing the 1D damage evolution.

In general compression, with Eqs. (14.1) and (14.2b), the damage variable is

$$D = \left(\frac{|F|}{H\varepsilon_s}\right)^n \tag{14.3a}$$

In general tension, with Eqs. (14.1) and (14.2a), the damage variable is

$$D = \left(\frac{|F'|}{H'\varepsilon'_s}\right)^{n'} \tag{14.3b}$$

in which ε'_s represents the strain when D=1 and here

$$H' = \frac{2(1+\nu)}{1+\alpha}, \quad H = \frac{2\alpha(1+\nu)}{1+\alpha}$$

The equation of the damage evolution is

$$\dot{D} = \frac{\partial D}{\partial \varepsilon} = \frac{n}{H\varepsilon_s}\left(\frac{|\dot{F}|}{H\varepsilon_s}\right)^{n-1} \quad \text{or} \quad \dot{D} = \frac{\partial D}{\partial \varepsilon} = \frac{n'}{H'\varepsilon'_s}\left(\frac{|\dot{F}'|}{H'\varepsilon'_s}\right)^{n'-1} \tag{14.4}$$

The experimental results of uniaxial and triaxial compression for sand-rock at the Jinchuan mine are shown in Fig. 14.6. The comparison of the calculated results based on the twin-shear damage model with the experimental results shows good agreement.

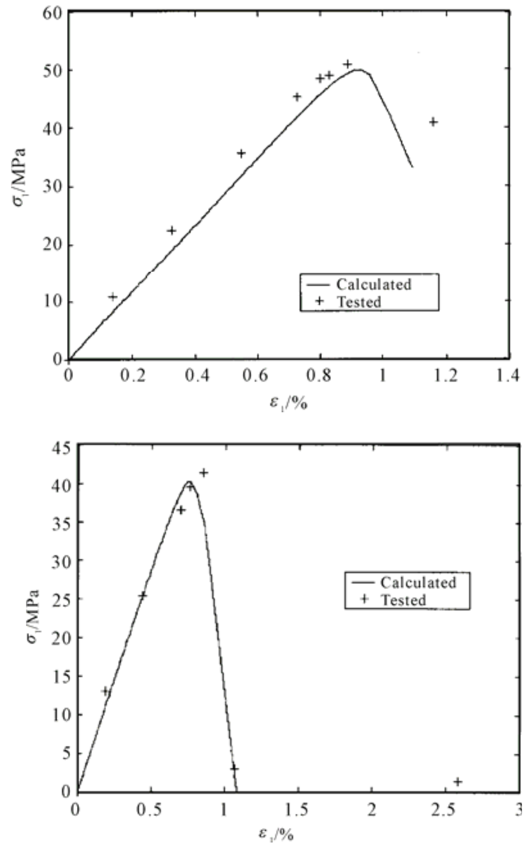

Fig. 14.6 Comparison of the twin-shear damage model with experimental results for sand-rock

14.3 Non-Equilibrium Iteration for Dynamic Evolution

At a certain loading step, damage and fracture of elements result in a decrease in the bearing capacity, which causes redistribution of stress in the structure. As a result, the stress around the damage zones increases. Furthermore, the elements around the damage zones will be damaged and fracture under the increased stress. This is the damage pattern and stress pattern coupling with each other; they are alternatively expanding and stopping. In the numerical method, the stress redistribution is carried out by non-equilibrium iterations.

At loading step k, the finite element equation is

$$K^{(k)}a^{(k)} = P^{(k)} \tag{14.5}$$

in which $a^{(k)}$ is the displacement array of step k; $P^{(k)}$ is node load array; $K^{(k)}$ is the overall stiffness matrix. It is assembled by the element stiffness matrix

$$K^{(k)} = \sum_e (K^{(e)})^{(k)} = \sum_e \int_{V_e} B^{\mathrm{T}} (D^{(e)})^e B \mathrm{d}V \tag{14.6}$$

in which B is the strain matrix, $(D^{(e)})^{(k)}$ is the element stiffness matrix of step k. It is expressed with the tensor as

$$(D^{(e)}{}_{ijkl})^{(k)} = (2G\delta_{ik}\delta_{jl} + \lambda\delta_{ij}\delta_{kl}) \tag{14.7}$$

in which G λ are Lame constants.

The non-equilibrium load result of element damage is

$$(K^{(k)} - \tilde{K}^{(k)})a^{(k)} = \Delta P^{(k)} \tag{14.8}$$

in which $\tilde{K}^{(k)}$ is the overall stiffness matrix because of damage at step k.

$$\tilde{K}^{(k)} = \sum_e (\tilde{K}^{(e)})^{(k)} = \sum_e \int_{V_e} B^{\mathrm{T}} (\tilde{D}^{(e)})^{(k)} B \mathrm{d}V \tag{14.9}$$

in which $(\tilde{D}^{(e)}_{ijkl})^{(k)}$ is the constitutive matrix of the damaged element. It is written as in tensors

$$(\tilde{D}^{(e)}_{ijkl})^{(k)} = (D^{(e)}{}_{ijkl})^{(k)}(1 - D^{(k)}) \tag{14.10}$$

Keep the load and boundary unchanged, approach equilibrium by iterative calculation and the stress is redistributed as

$$\tilde{K}^{(k)}\Delta a^{(k)} = \Delta P^{(k)} \tag{14.11}$$

The displacements are resolved as $\tilde{a}^{(k)}$

$$\tilde{a}^{(k)} \leftarrow a^{(k)} + \Delta a^{(k)} \tag{14.12}$$

The accumulated displacement is $\tilde{\varepsilon}^{(k)}$

$$\tilde{\varepsilon}^{(k)} = B\tilde{a}^{(k)} \tag{14.13}$$

Use Eqs. (14.2a) or (14.2b) and (14.3a) or (14.3b) for each element and calculate the damage value, then enter Eqs.(14.11)–(14.13). Repeat this course until no damage is produced. Then the step k calculation ends and the program enters the next step calculation.

14.4 Numerical Simulation of Caving Process Zone

14.4.1 Introduction to Block Cave Mining

Block cave mining is a mass mining method that allows for the bulk mining of large, relatively lower grade ore bodies. This method is increasingly being proposed for a number of deposits worldwide such as in Northparkes (Australia), Palabora (South Africa), Questa Mine (New Mexico), Henderson Mine (Colorado) and Freeport (Indonesia). In general terms block cave mining is characterized by caving and extraction of a massive volume of rock which potentially translates into the formation of a surface depression whose morphology depends on the characteristics of the mining, the rock mass and the topography of the ground surface (Fig. 14.1).

A major challenge at the mine design stage is to predict how specific ore bodies will react to block caving depending on the various geometry of the undercut. The scheme of undercut is the most feasible and creative factor because it can directly or indirectly change the cavibility of the ore body and decrease the rate of massive fragments. The caving process zone is the perturbation zone of the ore body above the free surface exposed by the undercut and ore drawing. It includes the caved zone and damaged zone (Fig. 14.2). It represents the dynamic characteristics of rock cracking, fracture and caving. In the chapter, a numerical simulation scheme for block cave mining for the Jinchuan Corp. Mine III (China) is introduced to give an illustration of the application of twin-shear strength theory in underground mining.

14.4.2 Geometry and Undercut Scheme

The experimental block is located in the south of the ore field (Fig. 14.7) and the size of the block and base structure is shown in Fig. 14.8a.

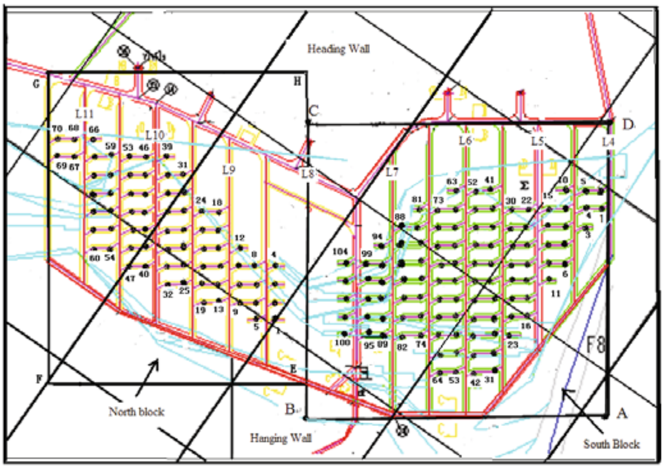

Fig. 14.7 Location of the experimental block (South block) in the ore field

The experimental block has a size of 180 m×140 m×188 m, with the highest level on the earth's surface and with the numerical boundary being 50 m from it. Stability of the base structure is not the aim. The undercut is divided into 6 equal paces which advance in the direction of positive *Y* (Fig. 14.8(b)). The velocity of the advancing undercut is determined by the principle that only if the ore body obtains transient stability at the previous pace will the next pace start.

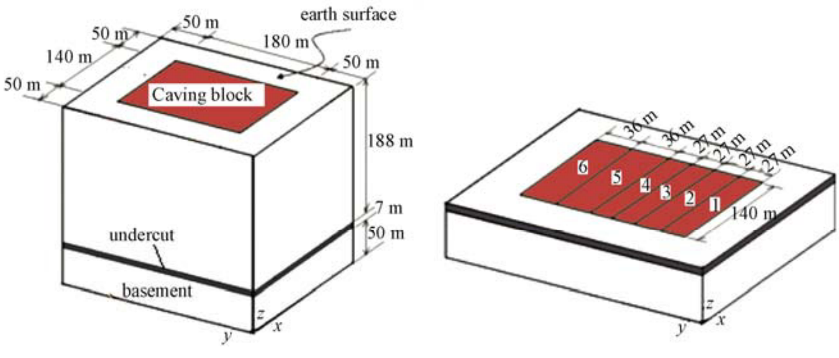

(a) Geometric model of the block mine

(b) The scheme of undercut

Fig. 14.8 The block and base structure and scheme of undercut

14.4.3 Result of Numerical Simulation

The finite element model is shown in Fig. 14.9, with its displacements set to zero except for the top surface.

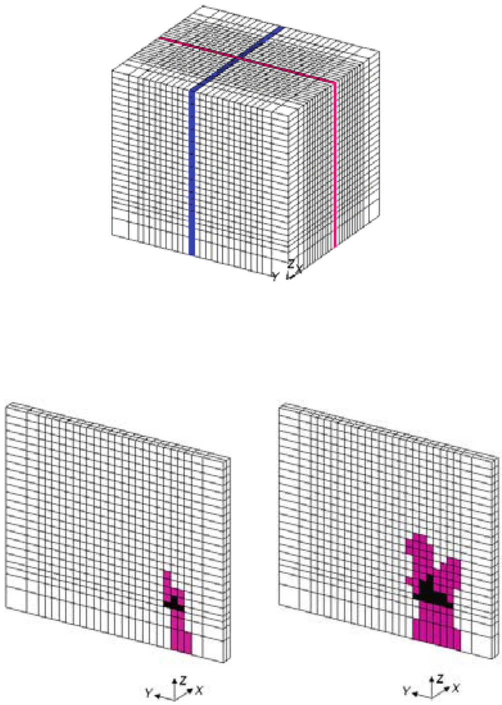

Fig. 14.9 The mesh of the block and undercut 1-1, 1-2

The elements attached to the middle plane of the model in the *X* direction are selected to show the evolution of the caving process zone, where the black elements represent the caved zone and the purple elements represent the damaged zone (Fig. 14.10). It shows that when the undercut 1 is finished, small caving occurs in the ore body. After the adjustment of stress, the damage zone expands but the caved zone does not, because the undercut pace is too slow. When the undercut 2 is finished, large scale caving occurs and the damage zone also expands much more, even if the undercut does not advance. So, from the undercut 3, the advance of the undercut goes fast and the next undercut should be carried out before the ore body stabilizes at the previous undercut, so that the subsequent undercut is carried out safely. At the end of the undercut, the process zone cannot retain a stable structure and continuous caving happens. Two large shear bands appear on the two sides above the caved zone.

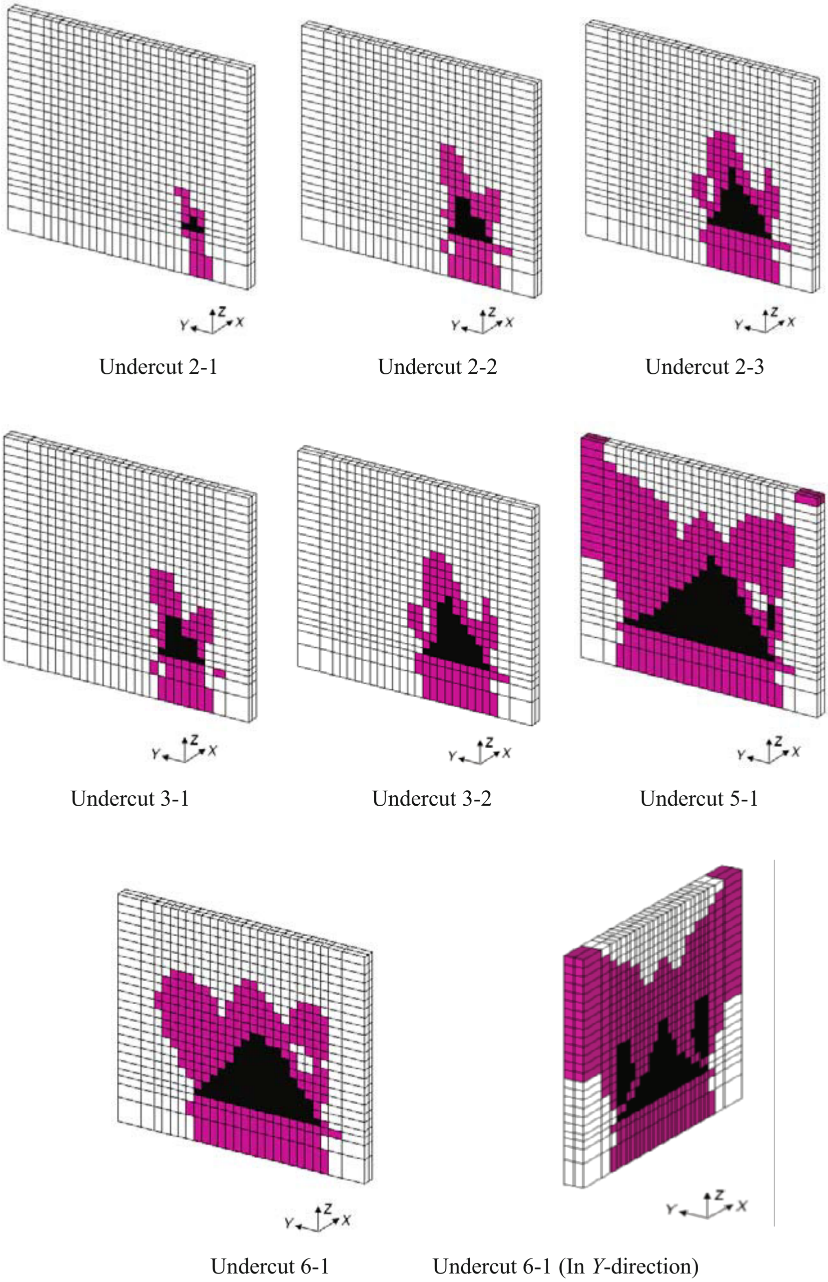

Fig. 14.10 Process zone evolution

14.5 Numerical Simulation for Crack Field Evolution in Long Wall Mining

14.5.1 Geometry and FEM Model

In this section we introduce the application of twin-shear strength theory in numerical simulation for crack field evolution in long wall mining in the Xinyi Coal Mine of the Yi Ma Coal Group in Henan province, China. The aim is to get a foreknowledge of pressure distribution on the workface and crack field evolution in the roof. The mechanical model is a plane strain in which the calculated plane is cross section I-I, as shown in Fig. 14.11 and Fig. 14.12. The FEM model is a fine mesh and rock strata are marked with different colors, as shown in Fig. 14.13.

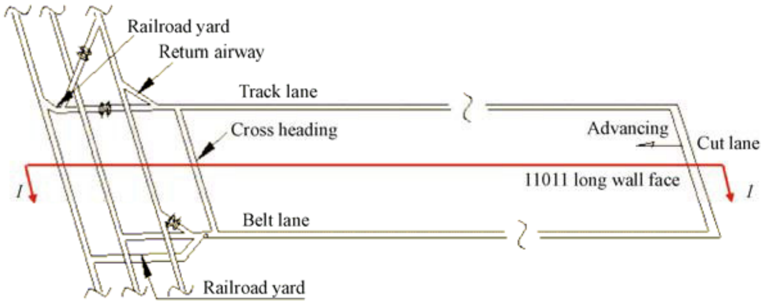

Fig. 14.11 Location of the calculated plane I-I

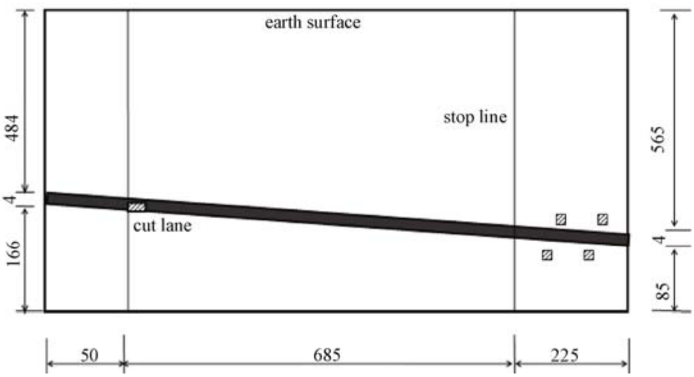

Fig. 14.12 Geometry of the cross section I-I

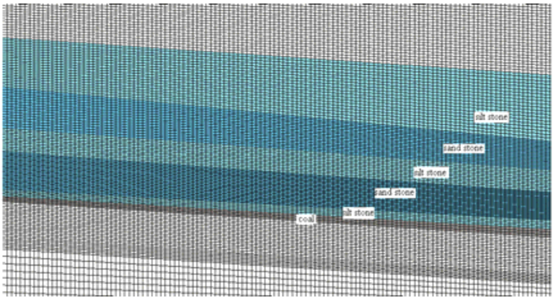

Fig. 14.13 Grid and distribution of rock strata in the calculated field

14.5.2 Evolution of Crack Field in the Roof

Part of the result is shown in Fig. 14.14. The orange color represents the worked-out section in the coal stratum and black represents the cracking zone.

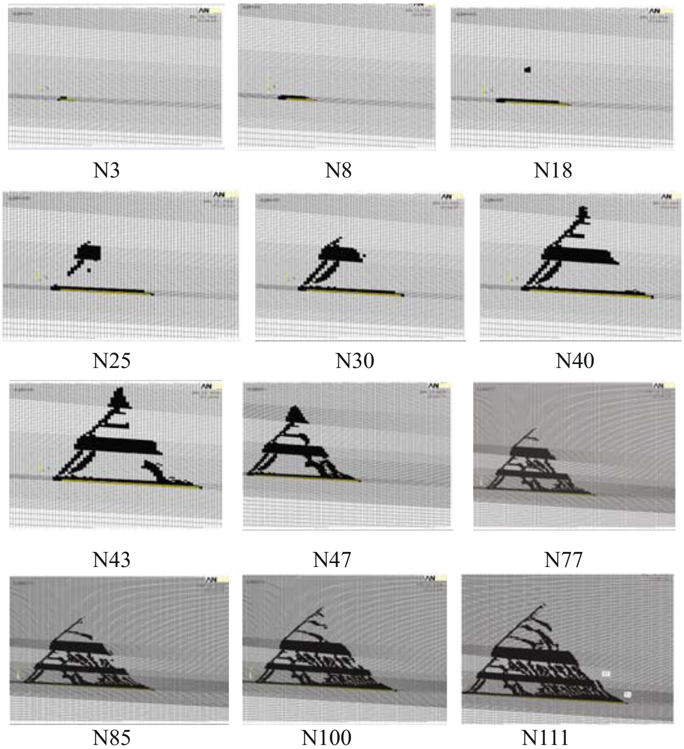

Fig. 14.14 Crack field evolution in roof

14.5.3 Results of Displacement and Stress

Contours of vertical displacement and principal stress σ_3 in the colorful strata are shown in Fig. 14.15. As the mining advances, the roof and the bottom of the worked-out section move oppositely. The largest displacement initially occurs at the main key stratum (K1) before K1 firstly breaks at N47. Then it goes upward as the inferior key stratum (K2) breaks firstly at N69 and, while the two key strata (K1 and K2) break periodically with the advance in the mining, it goes forward. Meanwhile, the zone in a state of tensile stress in the roof initially enlarges and then disappears. Instead, zero stress occurs and enlarges the roof with the breaking of the roof. The pressure on the two ends of the worked-out section will increase, as shown in Fig. 14.15 and Fig. 14.16.

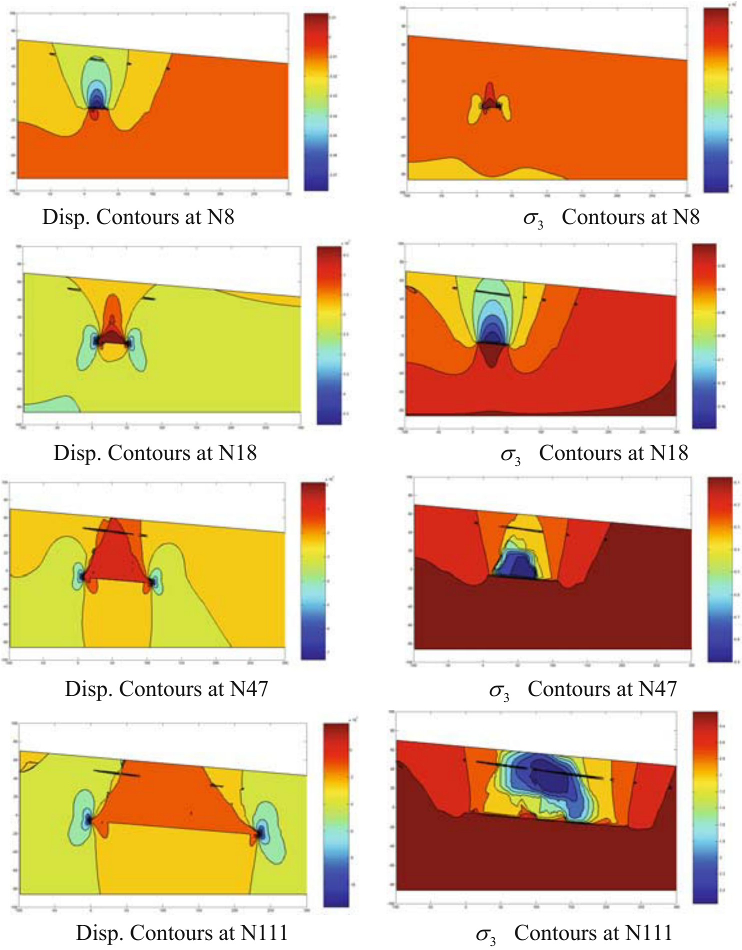

Fig. 14.15 Contours of displacement and stress

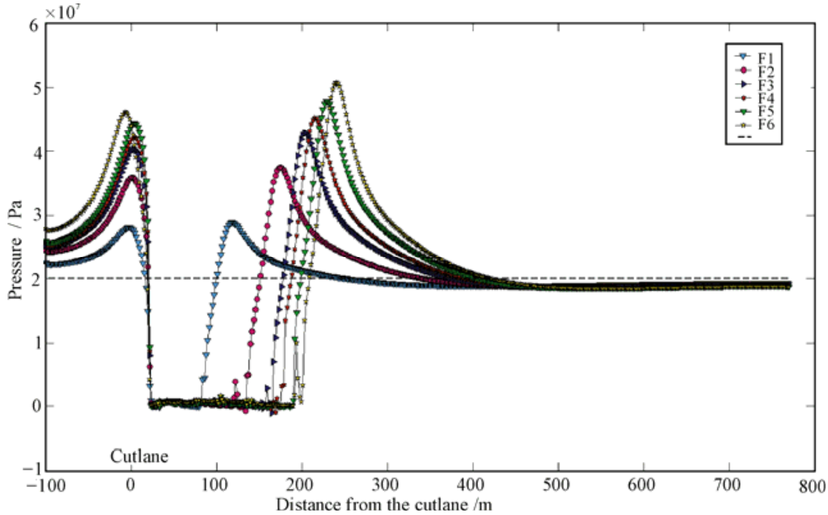

Fig. 14.16 Pressure distribution on the two ends of the worked-out section when K1 is breaking

In fact, with the strata in the roof breaking and caving, the opposite movement of roof and bottom will be prevented by the swelling rock and the zero stress zone will benefit from a supporting effect.

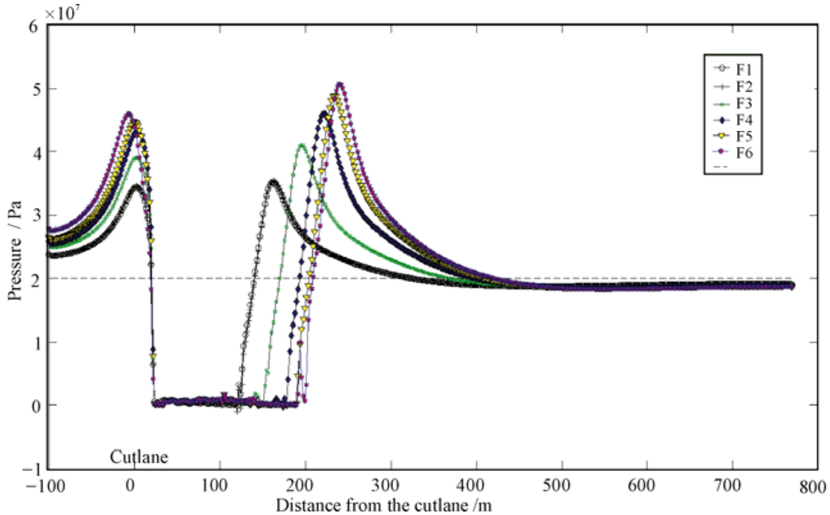

Fig. 14.17 Pressure distribution on the two ends of the worked-out section when K2 is breaking

References

Brown ET (2003) Block caving geomechanics. The international caving study I, 1997-2000. JKMRC monograph series in mining and mineral processing, University of Queensland, vol. 3. Indooroopilly, Australia: JKMRC.

Qian MG, Miu XX ,Xu JL et al. (2000) Key Strata Theory In Ground Control. China Mining and Technology University Press: Xu Zhou, China (in Chinese).

Yu MH, He LN, Song LY (1985) Twin shear stress theory and its generalzation. Scientia Sinica (Science in China, Series A), 28(11): 1174-1183 (English edn.); Chinese edn. ,28(12): 1113-1121.

Yu MH (1994) Unified strength theory for geomaterials and its application. Chinese Journal of Geotechnical Engineering, (2): 1-10 (in Chinese, English Abstract).

Yu MH (1998) Twin-Shear Theory and its Applications. Science Press: Beijing (in Chinese).

Yu MH (2004) Unified Strength Theory and its Applications. Springer: Berlin.

Zhou WY, Shan GR and Yang RQ (1998) Elasto-brittle damage model of rock and its applications. Chinese Journal of Geotechnical Engineering, 20(5): 54-57.

Wang L, Chen YJ and Gao Q (2009) Numerical simulation on caving process zone induced by undercut. Nonferrous Metals (Mining Section), 61(3): 44-48 (in Chinese).